

Experimental Study of a novel adaptive decision-directed channel equalizer in 28 GBaud RGI-DP-CO-OFDM transport systems

Mohammad E. Mousa-Pasandi,* Qunbi Zhuge, Xian Xu, Mohamed M. Osman, Mathieu Chagnon, and David V. Plant

Photonic Systems Group, Department of Electrical and Computer Engineering, McGill University, Montreal, QC, H3A-2A7, Canada

*me.mousapasandi@mail.mcgill.ca

Abstract: We report and experimentally investigate the performance of an adaptive decision-directed channel equalizer (ADDCE) in reduced-guard-interval dual-polarization coherent-optical orthogonal-frequency-division-multiplexing (RGI-DP-CO-OFDM) transport systems. ADDCE retrieves an estimation of the phase noise value after an initial decision making stage by extracting and averaging the phase drift of all OFDM sub-channels. Moreover, it updates the channel transfer matrix on a symbol-by-symbol basis. We experimentally compare the performance of the ADDCE and the conventional equalizer (CE) combined with maximum-likelihood (ML) phase noise compensation and inter-subcarrier-frequency-averaging (ISFA) algorithms. The study is conducted at 28 GBaud for RGI-DP-CO-OFDM systems with quadrature-phase-shift-keying (QPSK) and 16 quadrature amplitude modulation (16-QAM) formats. Using ADDCE, zero-overhead laser phase noise compensation is accomplished and the overhead due to training symbol (TSs) insertion is significantly reduced. In addition, ADDCE offers a superior performance over the CE in the presence of synchronization timing errors and residual chromatic dispersion (CD). We also achieve a longer transmission distance than when using the CE. At a forward-error-correction (FEC) threshold of 3.8×10^{-3} , using a cumulative overhead of less than 2.6%, transmission distances of 5500 km and 400 km were achieved for the cases of QPSK and 16-QAM RGI-DP-CO-OFDM, respectively.

©2012 Optical Society of America

OCIS codes: (060.4080) Modulation; (060.1660) Coherent communications.

References and links

1. W. Shieh, H. Bao, and Y. Tang, "Coherent optical OFDM: theory and design," *Opt. Express* **16**(2), 841–859 (2008).
2. W. Shieh, X. Yi, Y. Ma, and Q. Yang, "Coherent optical OFDM: has its time come?" *J. Opt. Netw.* **7**(3), 234–255 (2008).
3. M. E. Mousa-Pasandi and D. V. Plant, "Data-aided adaptive weighted channel equalizer for coherent optical OFDM," *Opt. Express* **18**(4), 3919–3927 (2010).
4. F. Buchali, R. Dischler, and X. Liu, "Optical OFDM: A Promising High-Speed Optical Transport Technology," *Bell Labs Tech. J.* **14**(1), 125–148 (2009).
5. S. L. Jansen, I. Morita, T. C. W. Schenk, N. Takeda, and H. Tanaka, "Coherent optical 25.8-Gb/s OFDM transmission over 4160-km SSMF," *J. Lightwave Technol.* **26**(1), 6–15 (2008).
6. X. Yi, W. Shieh, and Y. Tang, "Phase estimation for coherent optical OFDM," *IEEE Photon. Technol. Lett.* **19**(12), 919–921 (2007).
7. S. L. Jansen, I. Morita, N. Takeda, and H. Tanaka, "20-Gb/s OFDM transmission over 4,160-km SSMF enabled by RF-Pilot tone phase noise compensation," in *Optical Fiber Communication Conference*, OSA Technical Digest Series (CD) (Optical Society of America, 2007), paper PDP15.
8. M. E. Mousa-Pasandi and D. V. Plant, "Improvement of phase noise compensation for coherent optical OFDM via data-aided phase equalizer," in *Optical Fiber Communication Conference*, OSA Technical Digest Series (CD) (Optical Society of America, 2010), paper JThA10.

9. M. E. Mousa-Pasandi and D. V. Plant, "Zero-overhead phase noise compensation via decision-directed phase equalizer for coherent optical OFDM," *Opt. Express* **18**(20), 20651–20660 (2010).
10. J. Ran, R. Grunheid, H. Rohling, E. Bolin, and R. Kern, "Decision-directed channel estimation method for OFDM systems with high velocities," in *Proceedings of IEEE Vehicular Technology Conference*, (Institute of Electrical and Electronics Engineers, New York, 2003), 2358–2361.
11. M. Rim, "Optimally combining decision-directed and pilot-symbol-aided channel estimation," *Electron. Lett.* **39**(6), 558–560 (2003).
12. X. Liu and F. Buchali, "A novel channel estimation method for PDM-OFDM enabling improved tolerance to WDM nonlinearity," in *Optical Fiber Communication Conference*, OSA Technical Digest (CD) (Optical Society of America, 2009), paper OWW5.
13. X. Liu and F. Buchali, "Intra-symbol frequency-domain averaging based channel estimation for coherent optical OFDM," *Opt. Express* **16**(26), 21944–21957 (2008).
14. C. J. Youn, X. Liu, S. Chandrasekhar, Y. H. Kwon, J. H. Kim, J. S. Choe, D. J. Kim, K. S. Choi, and E. S. Nam, "Channel estimation and synchronization for polarization-division multiplexed CO-OFDM using subcarrier/polarization interleaved training symbols," *Opt. Express* **19**(17), 16174–16181 (2011).
15. S. Chen, Q. Yang, Y. Ma, and W. Shieh, "Real-time multi-gigabit receiver for coherent optical MIMO-OFDM signals," *J. Lightwave Technol.* **27**(16), 3699–3704 (2009).
16. X. Liu, S. Chandrasekhar, B. Zhu, P. J. Winzer, A. H. Gnauck, and D. W. Peckham, "448-Gb/s reduced-guard-interval CO-OFDM transmission over 2000 km of ultra-large-area fiber and five 80-GHz-grid ROADMs," *J. Lightwave Technol.* **29**(4), 483–490 (2011).
17. B. Spinnler, "Equalizer Design and Complexity for Digital Coherent Receivers," *IEEE J. Sel. Top. Quantum Electron.* **16**(5), 1180–1192 (2010).

1. Introduction

Following the recent surge of interest in digital signal processing (DSP) for optical fiber communications, coherent-optical orthogonal-frequency-division-multiplexing (CO-OFDM) has been intensively investigated as a possible modulation format for future uncompensated fiber optic transmission links. One of the key attributes of using DSP is the capability to send training symbols (TSs) and pilot subcarriers (PSCs) which are known to the receiver to provide data-aided channel estimation [1–3]. To combat dynamic changes in channel characteristics, i.e. polarization mode dispersion (PMD), and to provide synchronization, the TSs are periodically inserted into the OFDM data symbol sequence. TSs have to be sent at a speed that is much faster than the speed of significant channel fluctuations [3,4]. TS overheads of 2% to 5% are often reported for CO-OFDM transport systems [1–5]. The performance of coherent transmission systems are also known to suffer from laser phase noise which requires not only tracking on a symbol-by-symbol basis but also extra equalization. By using the PSCs that are inserted in every symbol, such fast time variations in the optical channel can be estimated and compensated [1,2,6]. An overhead of 3% to 5% is expected due to the PSC insertion [1–6]. In [5,7], the authors proposed RF-pilot enabled phase noise compensation for CO-OFDM systems with ideally no extra optical bandwidth. In this technique, phase noise compensation is realized by placing an RF-pilot tone in the middle of the OFDM signal band at the transmitter that is subsequently used at the receiver to revert the phase noise impairments. Inserting the RF-pilot typically results in a 10% power overhead [5,8].

Recently, we proposed in [3,9], two decision-directed equalizers for single-polarization CO-OFDM systems based on a combination of decision-directed and data-aided estimation schemes to increase the accuracy of channel estimation and to reduce the required overhead due to the TSs and PSCs [10,11]. In this paper, we adopt the same approach and experimentally demonstrate zero-overhead phase noise compensation via an adaptive decision-directed channel equalizer (ADDCE) for reduced-guard-interval dual-polarization coherent-optical orthogonal-frequency-division-multiplexing (RGI-DP-CO-OFDM) transmission systems. ADDCE, after an initial decision making stage, retrieves an estimation of the common phase noise value for the time interval of one OFDM symbol by extracting and averaging the phase drift of all OFDM sub-channels. It also updates the channel transfer matrix, initially acquired using TSs, on a symbol-by-symbol basis enabling the equalizer to increase the periodicity of the TSs and equivalently to reduce the TS overhead. The experimental results at 28 GBaud using both quadrature-phase-shift-keying (QPSK) and 16-quadrature-amplitude-modulation (16-QAM) formats confirm not only the feasibility of the zero-overhead phase noise compensation but also the superior bit-error-rate (BER) performance of the ADDCE versus a conven-

tional equalizer (CE) due to a more accurate channel estimation. At a forward-error-correction (FEC) threshold of 3.8×10^{-3} , transmission distances of 5500 km and 400 km were achieved for the case of QPSK and 16-QAM RGI-DP-CO-OFDM, respectively, using zero-overhead phase compensation and a cumulative overhead of less than 2.6%. We also study the effect of the synchronization timing error and the residual dispersion on the ADDCE and the CE and demonstrate the superior performance of the ADDCE. It is notable that since ADDCE operates on a symbol-by-symbol basis and considering that OFDM symbol rates can be much lower than the actual transmitted bit-rate, implementing ADDCE does not necessarily require very high-speed and high power consuming electronics. A brief analysis of the computational complexity of this scheme in terms of the number of required complex multiplications is provided, showing a complexity of only 28%.

This paper is structured as follows. We explain the ADDCE principles in section 2. In section 3, we experimentally study the performance of ADDCE in RGI-DP-CO-OFDM transport systems. In section 4, a brief analysis of the complexity of ADDCE is provided and section 5 concludes the paper.

2. ADDCE for dual-polarization transmission

Assume n and k denote the indexes for the received symbol (time index) and the OFDM subcarrier (frequency index), respectively. X and Y represent the two optical polarizations. In RGI-DP-CO-OFDM systems, the subcarrier-specific received complex value vector, $R_{n,k}$, is first sent to a static overlapped frequency-domain equalizer (OFDE) to compensate for the effect of CD. The resulting vector, $\hat{R}_{n,k}$, is then equalized by applying the zero-forcing technique based on the previously estimated transfer matrix, $\tilde{H}_{n-1,k}$, that is taken as a prediction of the current channel transfer matrix:

$$\begin{bmatrix} \hat{S}_{n,k}^X \\ \hat{S}_{n,k}^Y \end{bmatrix} = \begin{bmatrix} \tilde{H}_{n-1,k}^{XX} & \tilde{H}_{n-1,k}^{XY} \\ \tilde{H}_{n-1,k}^{YX} & \tilde{H}_{n-1,k}^{YY} \end{bmatrix}^{-1} \times \begin{bmatrix} \hat{R}_{n,k}^X \\ \hat{R}_{n,k}^Y \end{bmatrix} \quad (1)$$

where $\hat{S}_{n,k}$ is the subcarrier-specific equalized complex value vector. Matrix $\tilde{H}_{0,k}$ is initially derived by using the TSs that are inserted at the beginning of each block of OFDM data symbols as described in [12]. To partially mitigate the effect of noise, a low-pass filter (LPF) is applied on $\tilde{H}_{0,k}$. Vector $\hat{S}_{n,k}$ is then detected by the demodulator of the first decision making stage as

$$\bar{S}_{n,k} = \text{Decision} \left\langle \hat{S}_{n,k} \right\rangle \quad (2)$$

Presuming that the decision, vector $\bar{S}_{n,k}$, was correct and knowing the received vector after OFDE, $\hat{R}_{n,k}$, we can estimate the average phase drift due to the laser phase noise in the time interval of the n^{th} received OFDM vector as

$$\Delta\varphi_n = \frac{(\Delta\varphi_n^X + \Delta\varphi_n^Y)}{2} = \frac{\left(\sum_{i=1}^N \left(\arg \{ \hat{R}_{n,i}^X \} - \arg \{ \bar{S}_{n,i}^X \} \right) \right) + \left(\sum_{i=1}^N \left(\arg \{ \hat{R}_{n,i}^Y \} - \arg \{ \bar{S}_{n,i}^Y \} \right) \right)}{2 \times N} \quad (3)$$

where N is the total number of OFDM subcarriers. As one can see, (3) tries to extract the phase drift of the OFDM sub-channels in the time interval of the n^{th} received vector, assuming that the optical channel drift due to other impairments such as CD and PMD is negligible. This is a good assumption since CD and PMD variations are believed to be low-speed in

comparison to the typical CO-OFDM symbol rate [3,4]. Since the calculation of (3) is done after the decision making in (2), a fairly reliable initial equalization is necessary to prevent error propagation. In this technique, as long as the amount of rotation does not result in incorrect initial decision making for the majority of the constellation points in every received vector, the phase noise can be retrieved and compensated. As one can expect, ADDCE performance for dense constellation formats is more sensitive to the optical channel impairments. Therefore, for scenarios with relatively high laser phase noise and/or long symbol duration, this technique is not capable of proper phase noise compensation and might require the assistance of the PSCs or the RF-pilot to avoid error propagation, as been presented in [3,8]. Afterward, the equalized vector is sent to the final decision making stage

$$S_{n,k} = \text{Decision} \left\langle \hat{S}_{n,k} \times e^{-j\Delta\phi_n} \right\rangle \quad (4)$$

where vector $S_{n,k}$ is the subcarrier-specific detected complex value vector.

In addition, by using (1) and knowing the detected vector, $\bar{S}_{n,k}$, and the received vector after OFDE, $\hat{R}_{n,k}$, the ideal channel transfer matrix can also be estimated. However, the channel transfer matrix has four unknown arrays while (1) offers only two linear equations. By using the current and the previous symbol decisions, one can derive four set of linear equations and then find the unknown arrays. However, to reduce the complexity, we propose a new way to alternately update just two unknown arrays per received vector. For instance, for received data vector with even indexes ($\text{mod}(n,2) = 0$), we update $\hat{H}_{n,k}^{XY}$ and $\hat{H}_{n,k}^{YX}$ only by the common phase noise value of the corresponding time interval as

$$\hat{H}_{n,k}^{XY} = \tilde{H}_{n-1,k}^{XY} \times e^{j\Delta\phi_n} \quad \text{if } \text{mod}(n,2) = 0 \quad (5.a)$$

$$\hat{H}_{n,k}^{YX} = \tilde{H}_{n-1,k}^{YX} \times e^{j\Delta\phi_n} \quad \text{if } \text{mod}(n,2) = 0 \quad (5.b)$$

And then by using (5.a.) and (5.b.), we derive the $\hat{H}_{n,k}^{XX}$ and $\hat{H}_{n,k}^{YY}$ via (1)

$$\hat{H}_{n,k}^{XX} = \frac{\hat{R}_{n,k}^X - \tilde{H}_{n,k}^{XY} \times S_{n,k}^Y}{S_{n,k}^X} \quad \text{if } \text{mod}(n,2) = 0 \quad (5.c)$$

$$\hat{H}_{n,k}^{YY} = \frac{\hat{R}_{n,k}^Y - \tilde{H}_{n,k}^{YX} \times S_{n,k}^X}{S_{n,k}^Y} \quad \text{if } \text{mod}(n,2) = 0 \quad (5.d)$$

For received data vectors with odd indexes ($\text{mod}(n,2) = 1$), we update $\hat{H}_{n,k}^{XX}$ and $\hat{H}_{n,k}^{YY}$ only by the common phase noise value of the corresponding time interval as

$$\hat{H}_{n,k}^{XX} = \tilde{H}_{n-1,k}^{XX} \times e^{j\Delta\phi_n} \quad \text{if } \text{mod}(n,2) = 1 \quad (6.a)$$

$$\hat{H}_{n,k}^{YY} = \tilde{H}_{n-1,k}^{YY} \times e^{j\Delta\phi_n} \quad \text{if } \text{mod}(n,2) = 1 \quad (6.b)$$

And then by using (6.a.) and (6.b.), we derive the $\hat{H}_{n,k}^{XY}$ and $\hat{H}_{n,k}^{YX}$ via (1)

$$\hat{H}_{n,k}^{XY} = \frac{\hat{R}_{n,k}^X - \tilde{H}_{n,k}^{XX} \times S_{n,k}^X}{S_{n,k}^Y} \quad \text{if } \text{mod}(n,2) = 1 \quad (6.c)$$

$$\hat{H}_{n,k}^{YX} = \frac{\hat{R}_{n,k}^Y - \tilde{H}_{n,k}^{YY} \times S_{n,k}^Y}{S_{n,k}^X} \quad \text{if } \text{mod}(n,2) = 1 \quad (6.d)$$

We call the resulting channel transfer matrix, $\hat{H}_{n,k}$, a decision-directed channel transfer matrix. $\hat{H}_{n,k}$ corresponds to the time interval of the n^{th} received OFDM vector and consequently, includes not only the common-phase-error (CPE) information of the laser phase noise process but also any drift in channel response. A low-pass filter (LPF) is applied to $\hat{H}_{n,k}$ to suppress the high-frequency noise. To update the channel transfer matrix for the next received vector, we apply a simple recursive filtering procedure using both the previously estimated channel transfer matrix, $\tilde{H}_{n-1,k}$, and the ideal channel transfer matrix, $\hat{H}_{n,k}$. The recursion is performed independently for each subcarrier and a time-domain correlation is implicitly utilized. No channel statistics such as correlation function or signal-to-noise ratio (SNR) are needed. The subcarrier-specific channel transfer matrix for the n^{th} received vector can then be updated as

$$\tilde{H}_{n,k}^{XX} = (1-\gamma) \times \tilde{H}_{n-1,k}^{XY} \times e^{j\Delta\phi_n} + \gamma \times \hat{H}_{n,k}^{XX} \quad (7.a)$$

$$\tilde{H}_{n,k}^{YY} = (1-\gamma) \times \tilde{H}_{n-1,k}^{YY} \times e^{j\Delta\phi_n} + \gamma \times \hat{H}_{n,k}^{YY} \quad (7.b)$$

$$\tilde{H}_{n,k}^{XY} = (1-\gamma) \times \tilde{H}_{n-1,k}^{XY} \times e^{j\Delta\phi_n} + \gamma \times \hat{H}_{n,k}^{XY} \quad (7.c)$$

$$\tilde{H}_{n,k}^{YX} = (1-\gamma) \times \tilde{H}_{n-1,k}^{YX} \times e^{j\Delta\phi_n} + \gamma \times \hat{H}_{n,k}^{YX} \quad (7.d)$$

where γ is the weighting parameter and can take any value between 0 and 1. A small value of γ boosts the role of previously estimated channel transfer matrix, $\tilde{H}_{n-1,k}$, while conversely, a large value of γ increases the effect of decision-directed channel transfer matrix, $\hat{H}_{n,k}$. γ controls the recursion and can either be a fixed or an adaptive value [3,8]. In this study, we choose a fix γ value of 0.1.

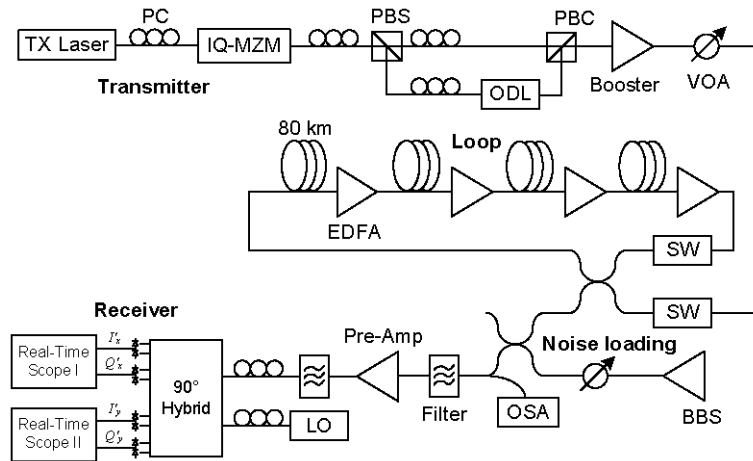


Fig. 1. RGI-DP-CO-OFDM experimental setup.

3. Performance of ADDCE in RGI-DP-CO-OFDM systems

In this section, we study experimentally the performance of ADDCE for both QPSK and 16-QAM RGI-DP-CO-OFDM transport systems. Figure 1 depicts the experimental setup. The original binary pseudo-random bit sequence (PRBS) data with the length of $2^{17}-1$ is first divided and mapped onto 112 frequency subcarriers with QPSK (16-QAM) modulation format and subsequently transferred to the time-domain by an IFFT of size 128 while zeros occupy the remainder, fixing the oversampling ratio of 1.14. In this RGI-DP-CO-OFDM system, a cyclic prefix of length 3 is employed, resulting in 2.34% of CP overhead. The CE employs 4 pilot subcarriers which can be translated in 3.57% of PSC overhead; however, ADDCE has no pilot subcarrier featuring the zero-overhead phase noise compensation. The CE and ADDCE use 2 training symbols (TSs) for every 100 and 1000 data symbols, equivalently 2% and 0.2% of TS overhead, respectively. This results in a cumulative overhead of ~8% (2.34% + 3.57% + 2%) and ~2.6% (2.34% + 0% + 0.2%) for the CE and the ADDCE, respectively. The in-phase (I) and quadrature (Q) parts of the resulting digital OFDM signal are then loaded separately on two field-programmable gate arrays (FPGAs) to electrically generate the electrical I and Q via two digital to analogue converters (DACs), operating at 32 GS/s. Using the oversampling ratio of 1.14, the analogue electrical I and Q signals at 28 Gbaud OFDM are generated and then fed into an IQ Mach-Zehnder modulator (IQ-MZM). After the IQ-MZM, a dual polarization emulator is used to imitate a dual-polarization multiplexed transmitter which results in 112-Gb/s and 224-Gb/s for QPSK and 16-QAM RGI-DP-CO-OFDM signals, respectively. The optical transmission link consists of a 4-span optical recirculating loop with uncompensated SMF with the dispersion parameter of 17 ps/nm.km, the nonlinear coefficient of $1.2 \text{ W}^{-1} \cdot \text{km}^{-1}$ and the loss parameter of 0.18 dB/km. Spans are 80 km long and separated by erbium-doped-fiber-amplifiers (EDFAs) with a noise figure of ~6 dB. At the optical receiver, two optical filters with bandwidths of 0.4 nm and 0.8 nm are applied before and after the preamplifier, respectively, to reject the out-of-band accumulated spontaneous emission (ASE) noise. The receiver is based on the intradyne scenario in which the received signal beats with the optical local oscillator (LO) signal in an optical polarization-diversity 90° hybrid to obtain the signal I and Q components. The LO is tuned to within the range of approximately tens of MHz of the received signal's center frequency. The four pairs of balanced outputs from the hybrid are then detected by four balanced photodetectors and then electrically sampled and asynchronously digitized at 80 GSamples/s using two commercial 4-channel real-time oscilloscopes, equipped with analog-to-digital converters (ADCs) characterized by 33 GHz of analogue bandwidth, a nominal resolution of 8-bit and a frequency-dependent effective number of bits (ENoB) between 4 and 5. Four signals are then transferred to PC for off-line processing. In the off-line processing section, to further characterize the capabilities of ADDCE, we compare the performance of the ADDCE with the CE combined with two other commonly-reported compensation schemes: the maximum-likelihood (ML) phase noise compensation [1,2] and the inter-subcarrier-frequency-averaging (ISFA) [13]. Throughout this study, the optimal ISFA parameter of 9 and 5 are adopted for the case of QPSK and 16-QAM formats, respectively. In our experiments in this paper, both the transmitter laser and the LO are commercial external-cavity-lasers (ECLs) with a nominal linewidth of 100 kHz.

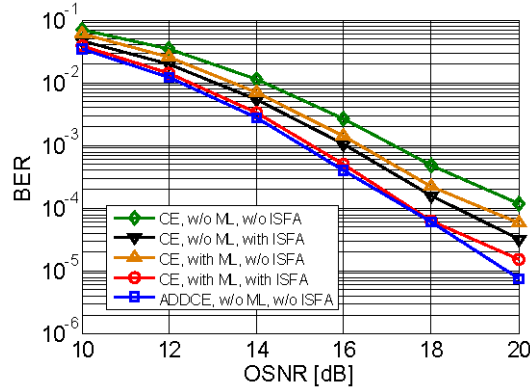


Fig. 2. BER vs. OSNR for 28 GBaud QPSK RGI-DP-CO-OFDM at optical B2B.

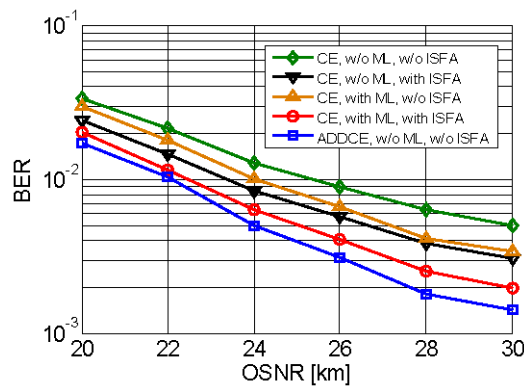


Fig. 3. BER vs. OSNR for 28 GBaud 16-QAM RGI-DP-CO-OFDM at optical B2B.

3.1. BER vs. OSNR and launch power

Figure 2 and Fig. 3 depict the BER versus optical signal to noise ratio (OSNR) for QPSK and 16-QAM RGI-DP-CO-OFDM, respectively. This measurement is performed in optical back-to-back (B2B) via a noise loading setup. We compare the performance of ADDCE versus the CE combined with and without ML and ISFA algorithms. As one can see, although ADDCE has zero-overhead phase noise compensation, it outperforms the CE throughout the OSNR range of study for both QPSK and 16-QAM RGI-DP-CO-OFDM. The CE combined with both ML and ISFA algorithms has the closest performance to the ADDCE. In Fig. 4 and Fig. 5, we characterize the performance of the equalizers versus launch power. The experiments are performed at the transmission distance of 3280 km and 328 km for QPSK and 16-QAM RGI-DP-CO-OFDM, respectively. As we see, ADDCE provides a superior performance and shows a similar behavior as the CE in noise- and nonlinear-limited regions.

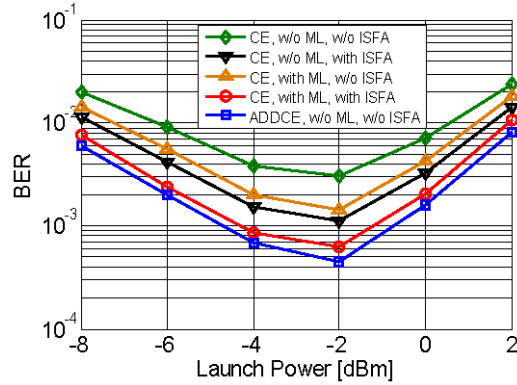


Fig. 4. BER vs. launch power for 28 GBaud QPSK RGI-DP-CO-OFDM at 3280 km.

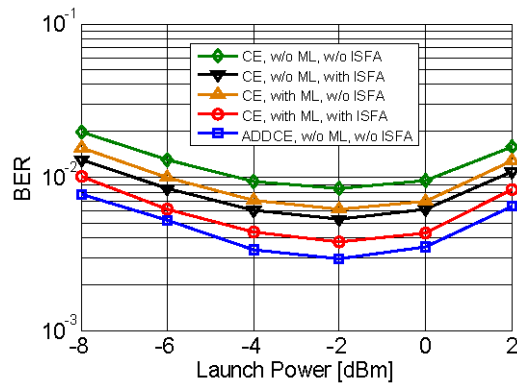


Fig. 5. BER vs. launch power for 28 GBaud 16-QAM RGI-DP-CO-OFDM at 328 km.

3.2. BER vs. synchronization timing error

In CO-OFDM, synchronization in time and frequency, are important and essential for DSP processes [14]. Synchronization timing error can degrade the performance of the equalization algorithms and are known to be sensitive in CO-OFDM systems [15]. In Fig. 6 and Fig. 7, we study the behavior of ADDCE and the CE with and without ML and ISFA algorithms in the presence of synchronization timing error for QPSK and 16-QAM RGI-DP-CO-OFDM, respectively. For the case of QPSK, this study is conducted at the transmission distance of 3280 km with an optical launch power of -2 dBm. For the case of 16-QAM, the transmission distance and the optical launch power were 328 km and -3 dBm, respectively. As seen for both QPSK and 16-QAM cases, the CE with ISFA algorithm are more susceptible to the synchronization timing error and the BER performance degrades dramatically which can be attributed to the effect of the inter-symbol-interference (ISI) on the inter subcarrier averaging. Moreover, since the optimal averaging parameter of the QPSK is larger than the 16-QAM, the degradation of the CE with ISFA in case of QPSK is more pronounced. Therefore, ADDCE demonstrates its superior performance as it is more robust than the CE with both ML and ISFA algorithms in the presence of synchronization timing error.

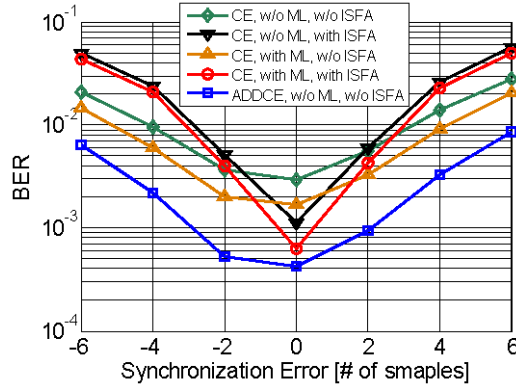


Fig. 6. BER vs. synchronization timing error for 28 GBaud QPSK RGI-DP-CO-OFDM at 3280 km.

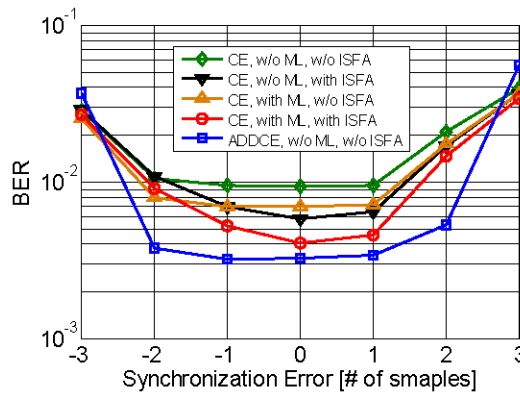


Fig. 7. BER vs. synchronization timing error for 28 GBaud 16-QAM RGI-DP-CO-OFDM at 328 km.

3.3. BER vs. residual dispersion

RGI-CO-OFDM systems are capable of reducing the cyclic prefix (CP) to compensate only for the ISI from the PMD and transmitter bandwidth limitations [16]. The essence of this approach is to compensate the CD by using a separate OFDE stage in prior to the OFDM channel estimation and demodulation. However, an accurate knowledge of CD is indispensable for an effective OFDE equalization. In Fig. 8 and Fig. 9, we study and compare the performance of the ADDCE and the CE in the presence of residual dispersion due to inaccurate CD estimation and/or equalization in OFDE for QPSK and 16-QAM RGI-DP-CO-OFDM, respectively. Similar to section 3.2., for the case of QPSK, the transmission distance and the optical launch power were 3280 km and -2 dBm, respectively. For the case of 16-QAM, the transmission distance and the optical launch power were 328 km and -3 dBm, respectively. As we see, the CEs with ISFA algorithms are vulnerable to residual CD and the BER performance degrades dramatically. This is because different OFDM subcarriers now experience different phase rotations due to residual CD and the averaging between neighbouring OFDM sub-channels in the ISFA algorithm results in inaccurate channel transfer matrix estimation. Similar to section 3.2., since the optimal ISFA averaging parameter for QPSK is larger than 16-QAM, the degradation of the CE with ISFA in case of QPSK is more pronounced. As one sees, ADDCE provides the same signal quality throughout the range of study, demonstrating its robustness to the effect of residual CD.

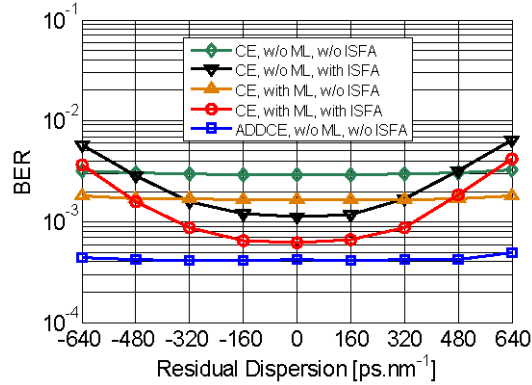


Fig. 8. BER vs. residual dispersion for 28 GBaud QPSK RGI-DP-CO-OFDM at 3280 km.

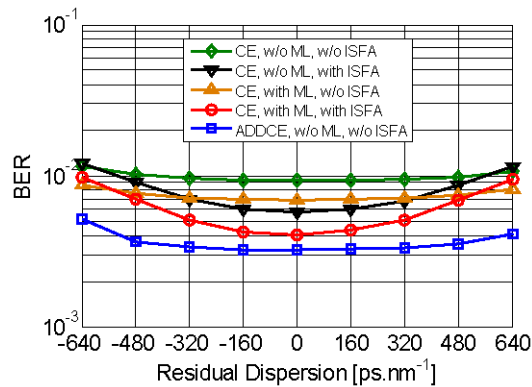


Fig. 9. BER vs. residual dispersion for 28 GBaud 16-QAM RGI-DP-CO-OFDM at 328 km.

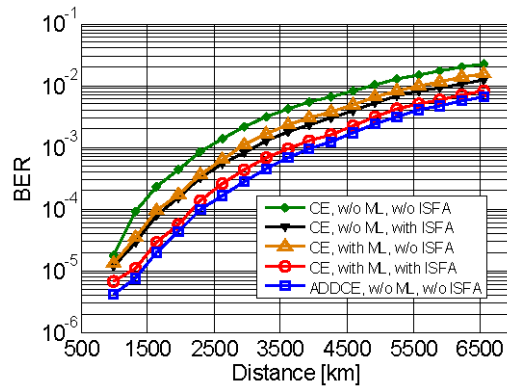


Fig. 10. BER vs. distance for 28 GBaud QPSK RGI-DP-CO-OFDM.

3.4. BER vs. transmission distance

In Fig. 10 and Fig. 11, we compare the BER performance versus transmission distance for the ADDCE and the CE combined with and without ML and ISFA algorithms for QPSK and 16-QAM RGI-DP-CO-OFDM, respectively. The optical launch power for QPSK and 16-QAM cases were -2 dBm and -3 dBm, respectively. As described earlier, the cumulative overhead for the CE is $\sim 8\%$. The ADDCE has a cumulative overhead of 2.6% featuring zero-overhead

phase noise compensation. As one can see, the ADDCE provides a better performance than the CEs. As we expect, the CE combined with both ML and ISFA algorithms has the closest performance to ADDCE. At the forward-error-correction (FEC) threshold of 3.8×10^{-3} , the ADDCE achieves a transmission distance of 5500 km and 400 km for QPSK and 16-QAM RGI-DP-CO-OFDM, respectively. These demonstrate 8% and 20% improvement in the transmission reach versus the CE with ML and ISFA algorithm for QPSK and 16-QAM RGI-DP-CO-OFDM, respectively. The ADDCE's capacity in overhead reduction, improving the transmission reach and resilience to the synchronization timing error and the residual dispersion, makes it an attractive alternative equalization algorithm.

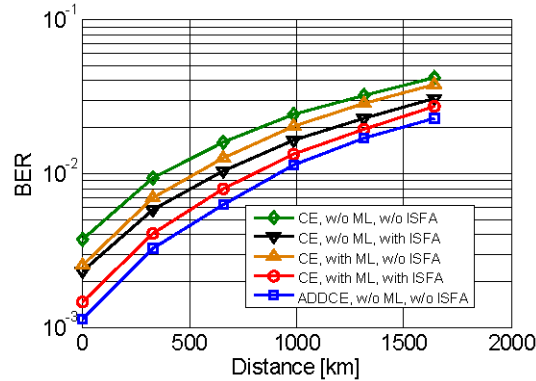


Fig. 11. BER vs. distance for 28 GBaud 16-QAM RGI-DP-CO-OFDM.

4. System complexity

The complexity of an equalization algorithm directly affects the implementation cost of the transmission link due to the hardware costs and power consumption. In this section, we provide a brief comparison of the complexity of the ADDCE and the CE, without ML and ISFA, in terms of the number of required complex multiplications per bit, taking into account the FFT operations, the channel estimation and equalization. In this study, the same complexity for multiplication and division is considered. Assume that the channel is estimated every N_{CE} symbols and R_{CE} is the training symbol overhead. M denotes the number of bits per symbol. As shown in [17], the complexity of the CE in an RGI-DP-CO-OFDM system, C_{CE} , can be expressed as

$$C_{CE} = \frac{N_1 (\log_2(N_1) + 1) n'_{MC}}{(N_1 - N_{CD} + 1) \log_2(M)} + \frac{n_{MC} \log_2(N_2) + 2 + \frac{5}{N_{CE} R_{CE}}}{\log_2(M)} \quad (8)$$

where N_1 , N_2 , n_{MP} and n'_{MP} are the FFT lengths of the first static frequency-domain equalization (FDE), FFT lengths of the second adaptive FDE, OFDM oversampling ratio and modified FDE oversampling ratio, respectively. N_{CD} represents the minimum number of equalizer taps necessary to compensate chromatic dispersion (CD) [17].

ADDCE has similar complexity regarding channel estimation however, six more complex multiplications, per used subcarrier for every polarization frame, are needed to implement Eq. (5) and Eq. (6). Furthermore, to derive Eq. (7), four more complex multiplications, per subcarrier per polarization frame, are required. To perform equalization, ADDCE updates the channel transfer matrix inversion of Eq. (1) on a symbol-by-symbol basis therefore, the complexity of a 2×2 matrix inversion, six complex multiplications per subcarrier per polarization

frame, needs to be considered. Assuming that every frame transmits $2N_2 \log_2(M)/n_{MC}$ bits then, the total complexity for ADDCE, C_{ADDCE} , is given by

$$C_{ADDCE} = \frac{N_1(\log_2(N_1)+1)n'_{MC}}{(N_1-N_{CD}+1)\log_2(M)} + \frac{n_{MC}\log_2(N_2)+2+\frac{5}{N_{CE}R_{CE}}}{\log_2(M)} + \frac{6N_2/n_{MC}+4N_2/n_{MC}+6N_2/n_{MC}}{2N_2\log_2(M)/n_{MC}} \quad (9)$$

$$= C_{CE} + \frac{8}{\log_2(M)}$$

For the case of the parameter of this experiment, we observe a complexity of 28% in terms of the number of complex multiplications.

5. Conclusions

We have summarized a series of experiments using a zero-overhead phase noise compensation based adaptive decision-directed channel equalizer (ADDPE) for 28 GBaud QPSK and 16-QAM reduced-guard-interval dual-polarization coherent-optical orthogonal-frequency-division-multiplexing (RGI-DP-CO-OFDM) transport systems. We compared the BER performance of the ADDCE and the conventional equalizer (CE) combined with maximum-likelihood (ML) phase noise compensation and inter-subcarrier-frequency-averaging (ISFA) algorithms. By comparing the ADDCE and the CE, we demonstrated that ADDCE can perform as reliably as the CE combined with both ML and ISFA algorithms. Transmission distances of 5500 km and 400 km over the uncompensated, EDFA-amplified transmission link were achieved for 28 Gbaud QPSK and 16-QAM RGI-DP-CO-OFDM, respectively whilst employing a cumulative overhead of less than 2.6%. Moreover, the ADDCE is more resilient than the CE to the effects of synchronization timing error and the residual dispersion.

Acknowledgments

The authors gratefully acknowledge the financial support from the Canadian Foundation for Innovation (CFI) and NSERC/Bell Canada Industrial Research Chair. Authors would like to thank Benoît Châtelain, Zhaoyi Pan, Ziad El-Sahn and Jonathan Buset for their fruitful help.